Image Correspondence With CUR Decomposition-Based Graph Completion and Matching

Sheheryar Khan, Mehmood Nawaz, Xu Guoxia, *Member, IEEE*, and Hong Yan, *Fellow, IEEE*

***Abstract*— Establishing correspondence between pictorial descriptions of two images is an important task and can be treated as graph matching problem. However, the process of extracting a favourable graph structure from raw images for matching is influenced by cluttered backgrounds and deformations, which may result in the abundance of noisy graph structures. This paper addresses the problem of point set correspondence and presents a robust graph matching method which recovers the correspondence matches among the graph nodes in a CUR based factorization framework. The graph representation in terms of CUR, inherently preserves the actual nodes connection in sparse manner, this particularly renders the complex space-time realization of affinities among graph nodes. The reformulation of graph matching in terms of small CUR factorization matrices, allows to compute and relax the partially observed graphs, without observing the whole large-scale graph matrix. In particular, we propose two variants of this approach, first, approximating the matching matrix from small CUR observed graph structure, and second, completing the graph structure with higher order CUR form to find correspondence. The CUR based matching algorithms are realized by computing set of compatibility coefficients from pairwise matching graphs and further conducting the probability relaxation procedure to find the matching confidences among nodes. Experiments and analysis on synthetic and natural images dataset prove the effectiveness of proposed methods against state-of-the-art methods. We also explore CUR matching for non-rigid moving object in a video sequence to demonstrate the potential application of graph matching to video analysis.**

***Index Terms*— Image correspondence, graph matching, CUR decomposition, non-rigid object matching.**

I. Introduction

ESTABLISHING correspondence among visual features in two images is critical for many applications, such as object matching and retrieval, action recognition, 2D and 3D image registration, and video analysis [1]–[4]. In a correspondence problem, it is generally assumed that key scene points are observable in images. The geometric structure in one image scene can be therefore correspondingly referred to other scene, resulting in matching key points along with deformations. The matching task is usually carried on geometric constraints over target space to find the best match by preserving the rich similarity measure.

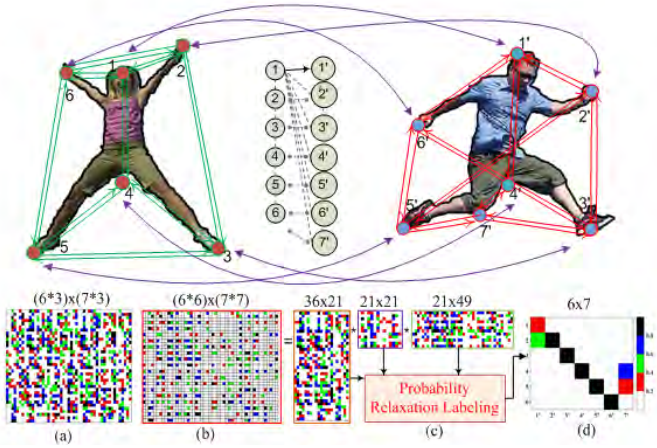

Fig. 1. An illustration of matching pair of human images having similar actions, with 6 and 7 features respectively. Compatibility coefficient matrix and its sampled version are shown below (a) represents bidirectional view of sampled edges, (b) Actual matrix, (c) represents the factorization in terms of CUR, sampling edges of graph 1, graph,2 and both along with relaxation labelling, (d) final assignment matrix.

For rigid point set matching, an estimation based framework such as iterative close point matching (ICP) [4] is employed to carry out the suitable correspondence among features. ICP algorithm is amongst the popular heuristic approaches, which assigns the correspondence by utilizing binary values, but the method is constrained to small scale planar deformations only. In contrast, Graph Matching (GM) [5]–[9] are effective to solve correspondence problems in images even for substantial deformations, as the information content from graph vertices and edges are strong enough to relate several objects in images. For example, the pair of images shown in Fig. 1 illustrates the matching of two humans with different pose and view geometry. The feature descriptor, in this case might be unsuitable to describe the correspondence relationship among them due to the similarities among nodes. However, graph matching with pair-wise relational information can be more effective under this situation. For example, distance and orientation coefficients can be used as scores among nodes in relation to the neighborhood to express symmetry.

Noteworthy, the underlying assumption of this correspondence geometrical information is based on whole affinity matches, and is achieved before modelling. However, many

Manuscript received April 30, 2019; revised July 18, 2019; accepted August 2, 2019. Date of publication August 16, 2019; date of current version September 3, 2020. This work was supported in part by the Hong Kong Research Grants Council under Project C1007-15G and in part by the City University of Hong Kong under Project 7005230. This article was recommended by Associate Editor W. Lin. *(Corresponding author: Sheheryar Khan.)*

The authors are with the Department of Electrical Engineering, City University of Hong Kong, Hong Kong (e-mail: sheheryar1984@gmail.com; mnawaz-c@my.cityu.edu.hk; guoxiaxu@cityu.edu.hk; h.yan@cityu.edu.hk).

Color versions of one or more of the figures in this article are available online at http://ieeexplore.ieee.org.

Digital Object Identifier 10.1109/TCSVT.2019.2935838

real applications implicitly relies on the prior node information. For example, feature point matching supposes the candidate points available from feature point extractor, but these unevaluated facts of extractor cannot guarantee the reliable matching. The assumption of initial setting potentially ignores noise and redundancy in nodes, edges or triangles (analogous to point-wise, pair-wise, triangles-wise). Therefore, initial assumption inevitably mixes the dummy nodes, deviated lines, even ambiguous combinations in assignment space. Furthermore, the issue in solving GM problem is the growth of node arrangement as a factorial paramount number with the graph dimension [10]. Under this scenario, the redundancy and computational complexity for pair-wise GM becomes intractable as the number of feature points increases [11], [12]. Alternate approaches are developed to overcome this problem by making a decent trade-off between computation complexity and accuracy.

Graph Laplacian or adjacency matrix in terms of eigen representation are adopted as an alternate in spectral methods, which makes them invariant subject to node arrangement [13]. For instance, eigen vectors as a global feature for point patterns are presented in [14] whereas in [6] eigen vectors are treated as correspondence indicators in matching. The eigen decompositions in the presence of positional jitter are likely to produce errors while computing eigen vectors whereas existence of outliers creates an additional challenge by making the size of graph size different. The proposed solutions to these issues truncated the eigenvectors to make them comparable, which later result in ineffectiveness of spectral representation.

Learning the compact affinity matrix of graph have been investigated frequently to realize robust feature correspondence [15]–[19]. The spectral matching method presented in [6] and local sparse models presented in [7] relaxed one to one matching constraint and later recovered back through post processing procedure. An interesting aspect of graph matching in terms of factorization was presented in [16]. The affinity matrix of graph was factorized into Kronecker product of smaller matrices that captures the affinities between the nodes and edges, and later convex-concave relaxation was carried out in path following fashion. Another method [15] exploit the matrix decomposition to extract the common inliers and their synchronized permutations from disordered weighted graphs in the presence of deformation and outliers.

Despite several attempts to realize GM in terms of decompositions [17], [18], [20], [21], the robustness and viability of many algorithms remain critical. The key step in graph structure analysis is to construct a compressed representation of affinity matrix that may be lighter to analyse. This is achieved by truncating at some value in larger part to yield best rank-k approximation of matrix when measured against any unitarily invariant matrix norm. Unfortunately, the basis vector-based approximations are notably difficult to interpret in terms of the actual graph structure, i.e. actual nodes and edges. In other words, the exact relaxation-based solutions of graph matching problem ignore the scalability.

Consequently, the corresponding geometrical structures could be naturally treated as an incomplete structure according to above noisy challenges. This is the main intuition that led us to introduce the approximation by randomization method rather than full or complete structure in graph. Here, the globally optimal solution cannot be easily achieved by several factors. Of all that, the most important barrier is the scale of the huge searching space. Based on incomplete assumption, we exploit a probabilistic model over matching space to cope with graph matching problem. In this case, we intuitively exploit the CUR decomposition method, which are relatively contemporary interpolative approaches and can deliver low-rank approximations in terms of actual graph connections that are more amenable to interpret as compared to linear combinations.

In this paper, we present a CUR decomposition based graph matching framework for image correspondence problems. The key idea behind the proposed method is to carefully sample the pairwise affinity graph matrix by keeping all the nodes of graph and without touching the whole graph matrix. The fact can be visualized in Figs. 1(a) to 1(d). The two-dimensional sampling results into a set of small matrices, i.e. C, U and R that capture the individual local graph structure, which offers several advantages over traditional low rank approximations in terms of computational complexity, storage and interpretation. For instance, to match a large number of points, the size of graph matrix tends to increase significantly. In this case, the sampled matrices in terms of C, U and R, are much easier to compute, store and process rather than accessing the whole larger affinity matrix with all possible combinations. As the affinity matrix is sparse and non-negative, the small factor matrices tend to share the similar properties. This makes them suitable for a label assignment procedure to reduce local ambiguities and achieve global consistency. Results into a set of small matrices, i.e. C, U and R that capture the individual local graph structure, which offers several advantages over traditional low rank approximations in terms of computational complexity, storage and interpretation. For instance, to match a large number of points, the size of graph matrix tends to increase significantly. In this case, the sampled matrices in terms of C, U and R, are much easier to compute, store and process rather than accessing the whole larger affinity matrix with all possible combinations. As the affinity matrix is sparse and non-negative, the small factor matrices tend to share the similar properties. This makes them suitable for a label assignment procedure to reduce local ambiguities and achieve global consistency.

Contributions: The main contributions of this work presented on graph matching for image correspondence can be summarized as follows:

1: To address the scalability issues related to graph matching, we propose to perform a bidirectional uniform graph matrix sampling, along rows and columns. We present the low-rank CUR decomposition for graphs and then relate it to solve the correspondence problem of matching images.
2: We propose two different variants of our approach related to graph decomposition which include (a) direct low-rank representation, and, (b) recovered low-rank representation. For direct low-rank representation, we use uniform sampling on compatibility coefficients scores matrix and reformulated the relaxation labelling that require only

a small number of combinations to process. In recovered low-rank representation, we extend the CUR decomposition to a tensor form and within the relaxation framework. We recover the tensor slices from its sampled low-rank components. The scheme is proved to be memory efficient as well as robust against deformations.

3: Through several experiments on synthetic and real data we validate the effectiveness of our proposed methodology, while addressing the aforementioned shortcomings.

II. Related Works

A. GM and Factorization

In graph matching, several pioneering works focused on heuristics and approximation based strategies. In general, the combinative characteristic of GM demands approximate solutions, as the global optimum can hardly be obtained. In this section, we will discuss selected approaches related to our research.

In context of graph matching, an incomplete list of classical approaches can be categorizes in to spectral methods [6], probabilistic approaches [9], tree search based methods or path following methods [16], [22]. Spectral methods tend to study the similarities among the spectra related to adjacency matrix or Laplacian matrix of graph, whereas the probabilistic methods conduct probability distributions that define mappings and then optimize over several constraints to yield refined match. In comparison the tree-search based methods usually have higher computational cost, generally of the exponential order, as they carry out sequential procedures of compatibility belonging to local graph structures.

Learning the pair-wise affinity matrix form graph and devising improved approximations of graph structure dual decomposition framework was followed in [17] to achieve the lower-bound on energy, which addressed dual of the matching problem [23]. However, the encoding may be susceptible to noise, making it sensitive to scaling and rotation changes. To overcome these shortcomings, the higher order extension was presented [10], [23], which encodes the geometric structure of graph in tensor form. However, any change in order of relations produced an enormous amount of data computation, therefore the method is limited only to sparse structures with third order only. The performance in this case is also dependent on the initial graph construction. Among these approaches, the aspect of graph matching via graph decomposition was better addressed in [16], in which factorization of affinity matrix was dealt directly. The smaller matrices were further relaxed through convex-concave procedure using path-following approaches.

Aiming to construct a compact parts-based representation from graph, non-negative matrix factorizations (NMF) gained much popularity in graph matching [20], [24]. Non-negative Orthogonal Graph matching (NOGM) presented in [20], which encoded the discrete mapping constraints of matching into nonnegative orthogonal constraints and then final solution is achieved through multiplicative updated fashion. The sparse solution from NNMF in this case is much easier to incorporate in optimization process. However, it fails to extract the intrinsic geometric and discriminating structure of actual data space, as the learning is carried out in Euclidean space [25].

Deep learning for graph matching is introduced in [26] to extract the image features using the convolution neural network (CNN) and learning the matching function of similarity, whereas inverse gradient propagation and standard CNN gradient optimization methods were adopted to achieve end-to-end training in CNN architecture. The method benefitted from the potential of deep learning to extract the key visual features in images instead of handcrafted features such as SIFT and then similarity matrix is constructed. The matrix is further passed to existing GM algorithm, for which the training loss is computed along with matched supervisory information. The process still combines the information of all nodes and edges to construct the graph and therefore overlook the sparsity of the affinity matrix.

Moreover, the eigen decomposition of the affinity matrix was used that requires the whole affinity matrix and basis vector approximations are notably difficult to interpret in terms of the actual graph structure. On contrary the proposed CUR based method is based on sampling the actual graph structure from affinity matrix and provides a sketch that is beneficial in in terms of interpretability and robustness against non-rigid nature of graph. The direct representation of data in terms of sampled factor matrices in CUR representation can be suitable in network compression such as weight quantization and weight sampling from convolution layers and fully connected layers for compact representations of CNN layers.

B. CUR Factorization

Nevertheless, interesting results can be seen in aforementioned literature, particularly in image matching problems, as they strictly emphasize on improving optimization strategies, but does not address the scalability issues in principle way, i.e., how to construct, store and process the large graphs over points in images. In contrast to these methods, our approach directly establishes factored matrices while partially observing the graph in randomized manner using the CUR decomposition.

As an alternate to the SVD type approximation, CUR decomposition is well acknowledged in data science to approximate the massive matrices in less memory and time requirements [27]–[30]. The author in [29] discussed the complexities related to computing the low rank structure of matrix in terms of CUR decomposition. The most popular Nystrom method to construct the matrix sketch using the uniform sampling and leverage score sampling [31] are commonly employed. In [29] the author discussed an effective way to compute the CUR decomposition as compared to Nystrom method. There are several recent papers of interest that shows more efficient ways to compute the CUR decompositions and its higher order generalizations [32], [33]. However, no graph matching aspect is involved.

The literature discussed above considered the numerical aspect of CUR decomposition, different problem than graph matching. Nevertheless, it does provide the underlying principle to conduct CUR decomposition in a much faster way.

In this paper, we followed the similar formulation as described in [29] to compute CUR decomposition and proposed a direct graph matching strategy that combines the compatibility matrix sketch from graph using the uniform sampling between edges. The factorization process involved here provides two key advantages as compared to previous methods. Firstly, the computation of large compatibility matrix is no longer necessary, instead small factor matrices are generated using partially observing the graph. This allows lower computation and memory requirements as compared to standard eigen value decomposition approaches, thus the problem of matrix inversion in case of large number of feature points can be dealt more efficiently. Secondly, the small sized actual entries present in factor matrices represent the actual graph structure, which enables the optimization process to converge more rapidly with few iterations.

III. Problem Statement

Given two graphs $G_1 = (V_Q, E_Q)$ and $G_2 = (V_Q{}', E_Q{}')$ from feature extracted images. Where $V_Q = \{q_1, q_2, \ldots, q_n\}$ and $V_{Q'} = \{q'_1, q'_2, \ldots, q_{m'}\}$ are the sets of nodes, whereas E'_Q and $E_Q{}'$ are the sets of edges. The task of image correspondence via graph matching is to obtain a mapping : $V_Q \rightarrow V_Q{}'$, such that the geometric structure between two graphs is retained. The graph structure can be denoted as $S = \{S_1, S_2, \ldots, S_l\} \in G_1$ and $S' = \{S'_1, S'_2, \ldots, S'_l\} \in G_2$ respectively. Here l represents the number of structures in graphs such that for any $l \leq \theta \leq l, \in S$ or $S_\theta{}' \in S'$ represents the points or edges as:

$S_\theta = \{q_{\theta 1}, q_{\theta 2}, \ldots, q_{\theta t}\}$ and $S_{\theta'} = \{q_{\theta 1'}, q_{\theta 2'}, \ldots, q_{\theta t'}\}$ where $l \leq t \leq T(T = min\{m, n\})$ represents the dimension of graph structure and possible graph structure in terms of patterns can be interpreted as $1 \leq l \leq \binom{T}{t}, q_{\theta T}$ and $q'_{\theta T}$ for $1 \leq T \leq t$ are the spatial points in both graphs V_Q and $V_{Q'}$ respectively.

Considering $F_{S\theta}$ and $F_{S\theta'}$ be features representing points from selected graph structure $S_\theta \in G_1$ and $S_{\theta'} \in G_2$, respectively.

$$Score = \sum_{(q\theta, q'\theta T) \in c} = f(F_{S\theta}, F_{S'\theta}), \tag{1}$$

where the target is to obtain the set of correspondence between graphs as $= \{(q_{\theta T}, q'_{\theta T}) | q_{\theta T} \in V_Q$ corresponding to $q'_{\theta T} \in V_{Q'}, 1 \leq \theta \leq l, 1 \leq T \leq t\}$. Usually the $f(F_{S\theta}, F_{S'\theta})$ are expressed in terms of distance measure or on compatibility scale, the cost function in former case becomes a minimization problem whereas in later case set as maximization problem. The final matching assignment t in terms of indicator vector takes the form as:

$$x(a) = \begin{cases} 1, & \text{if } a = (q_{\theta T}, q'_{\theta T}) \in C \\ 0, & \text{otherwise} \end{cases} \tag{2}$$

where $(q_{\theta T}, q'_{\theta T}) = 1$ represents that node $q_{\theta T}$ matches node $q'_{\theta T}$. The final assignment matrix can be discretized to [0 1]. Suppose the pair-wise case, the minimizing objective function Eq. (1) have a same effect with matching probability. In general, the matching problem can be solved by maximizing the probability. In discrete domain, the intuitional solution is provided by maximizing the probability of assignment matrix and can be defined on:

$$\hat{X} = \arg\max_X (score) \tag{3}$$

The task here is to maximize the number of matched edges between two graphs. The correspondence between sets of edges is represented by a compatibility matrix f and each element of f has a continuous value i.e [0 1]. The matching is achieved by maximizing the score function by probability relaxation labelling (PRL) method, which is an iterative process to reduce ambiguities in assignment labels. The set of matching probabilities are assigned initially and are then updated by PRL process. The overall task is to achieve a maximized matching score, under the relaxed condition of probability as $P_{q\theta T q'\theta T} \in$ [0,1]. At the end of PRL process, it is expected that each node will have one unambiguous probability that constructs the final matching matrix.

The optimization problem in Eq. (3) is NP-hard and there exists variety of approaches [9], [22], [23] to solve it. In fact, it becomes more critical when the graph size is relatively large, and the factorial growth of graph structure makes it practically more challenging. The section below describes the proposed randomized approach to deal with the issue and realize the solution based on CUR decomposition with probability relaxation labelling.

IV. Proposed GM Framework

We solve the image correspondence problem by computing the set of compatibility coefficients from the pair-wise graph representing the feature points. Once the compatibility scores are computed from graphs, it is then passed to the relaxation labelling process to solve the optimization problem. The factorial indexed terms involved in compatibility matrix and an exhaustive iterative search in this case is computationally intractable even for moderate sized graphs. Thus, we propose an efficient CUR decomposition based strategy to compute and solve the relaxation problem in following key steps:

- Compute and store only the partially observed graph structure in terms of factors matrices to realize compatibility scores.
- Search the relaxation labelling process over small low rank graph structures to generate the assignment matrix. These following subsections elaborate the points.

A. Compatibility Measures

The rich contextual information present in the graph structures can be described in terms of compatibility coefficients [9], [34]. Distance among pairs of points is one of the most commonly used measure to describe the similarity, but for deformable objects this might not be suitable alone. Whereas the angle information sufficiently preserves the topology of shapes, even the points are distorted, as the neighborhood structure of the points is retained. Based on these assumptions we used both distance and angle information among pairwise graph structure to encode the compatibility

coefficient information. Considering the nodes of graphs with single indexing to represent the points in two sets, the graph structure can be represented in terms of points as:

$q_i \in V_Q$ $(i = 1, 2, 3 \ldots, n)$ and $q'_\lambda \in V'_Q$ $(\lambda = 1, 2, 3 \ldots, m)$ from G_1 and G_2 respectively.

The overall compatibility measure of pair-wise graph structure is represented by a coefficient $C_{q_i q_j}(q'_\lambda, q'_\eta)$ where the-subscript terms represents the pairs in object set whereas the terms in bracket corresponds to target set, such as: $(i, j = 1, 2, 3 \ldots, n)$ and $(\lambda, \eta = 1, 2, 3 \ldots, m)$ Each coefficient represents the potential to match a pair $a = (q_i, q'_\lambda)$ with pair $b = (q'_j, q'_\eta)$ The Euclidean distance compatibility coefficient can be given by:

$$D_{qiqj}(q'_\lambda, q'_\eta) = 1 - |\frac{d(q_i, q_j) - d(q'_\lambda, q'_\eta)}{d(q_i, q_j) + d(q'_\lambda, q'_\eta)}| \tag{4}$$

where $d(q_i, q_j)$ is the distance between pairs q_i and q_j of V_Q whereas $d(q'_\lambda, q'_\eta)$ is the distance between pairs q'_λ and q'_η of V'_Q. The value of coefficient lies in the range from 0 to 1 depending upon how closely the pairs are similar, e.g, $D_{qiqj}(q'_\lambda, q'_\eta)$ is 1, if $d(q_i, q_j)$ and $d(q'_\lambda, q'_\eta)$ are equal alternatively close to zero when when $d(q_i, q_j) \gg d(q'_\lambda, q'_\eta)$ or $d(q_i, q_j) \ll d(q'_\lambda, q'_\eta)$ The angle coefficient is computed from each pairs of points in terms of the dot product as

$$A_{qiqj}(q'_\lambda, q'_\eta) = \left(1 + \frac{\overrightarrow{q_1 q_j} . \overrightarrow{q'_\lambda q'_\eta}}{\|\overrightarrow{q_1 q_j}\| . \|\overrightarrow{q'_\lambda q'_\eta}\|}\right)/2 \tag{5}$$

where $\overrightarrow{q_1\ q_j} . \overrightarrow{q'_\lambda q'_\eta}$ represents the dot product between two vectors and the amplitude scale is denoted by $\|\overrightarrow{q_1\ q_j}\|$ and $\|\overrightarrow{q'_\lambda q'_\eta}\|$. For the pair of vectors $\overrightarrow{q_1\ q_j}$ and $\overrightarrow{q'_\lambda q'_\eta}$ the orientation angle $\theta \in [0, \pi]$ then the corresponding coefficient $A_{qiqj}(q'_\lambda, q'_\eta)$ ranges between 1 and 0 respectively. The above explained coefficients based on distance and orientation can be combined to form a resultant position coefficient as:

$$C_{qiqj}(q'_\lambda, q'_\eta) = A_{qiqj}(q'_\lambda, q'_\eta) . D_{qiqj}(q'_\lambda, q'_\eta) \tag{6}$$

The resultant coefficient determines the overall compatibility of matching any point q_i with q'_λ and q_j with q'_η along with value also ranging between 0 and 1.

B. Relaxation Labelling

The optimization problem presented in Eq. (3) can be dealt with the relaxation labelling procedure incorporating the position compatibility coefficient. To serve the purpose of graph matching, the relaxation labelling procedure maps each point from an initial set to target set while iteratively reducing the ambiguities in assignment labels, therefore achieves the global consistency [28]. The procedure is initialized by assigning an initial matching probability and is then updated iteratively, based on the support function. The subsequent process assigns or updates the matching probability that maximizes the cost function. It is therefore assumed to have an explicit matching probability in assignment matrix at the end of procedure, where no further improvement can be seen afterwards.

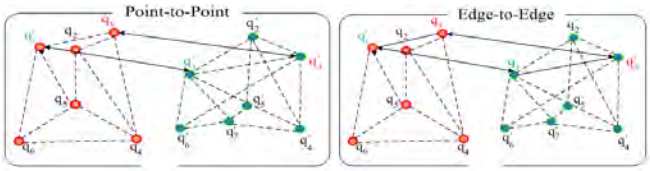

Fig. 2. The description of graph structure dimension. When dimension is 1, the process becomes point to point matching, matching.

Considering pairwise graph matching the structure dimension is set to 2 and $1 \leq \theta \leq l$ the graph structure $S_\theta = \{q_{\theta 1}, q_{\theta 2}\} \in V_Q$ must correspond to the labels in V'_Q as $S'_\theta = \{q'_{\theta 1}, q'_{\theta 2}\} \in V_{Q'}$. Referring to Fig. 2, the task becomes matching q_{q1} with $q'_{\theta 1}$ and q_{q2} with $q'_{\theta 2}$ with corresponding labels. The prior probability for matching is set to initialize the relaxation process. For $q_1 \in V_Q$, the prior probability can be stated as: $p^{(0)}_{qi \to q'_\lambda}$ $(0 \leq p^{(0)}_{qi \to q'_\lambda} \leq 1)$ to match corresponding label $q'_\lambda \in V_{Q'} (0 \leq \lambda \leq m)$ while satisfying the unity sum criterion as: $\sum_{\lambda=1}^{m} p^{(0)}_{qi \to q'_\lambda} = 1$.

For the compatibility coefficient $C_{qiqj}(q'_\lambda, q'_\eta)$, it follows the high matching probability among $q_i q_j$ and $q'_\lambda q'_\eta$ if the score is closer to one and incompatible if it is closer to zero. There is the support function T_{qi}, derived from the compatibility coefficient and weight factor of initialized probability, that represents the scale of each q_j cpmbined with q_i for label q'_λ.

$$T_{qj} \leftarrow \sum_j \sum_\eta C_{qiqj}(q'_\lambda, q'_\eta) p^{(0)}_{qi \to q'_\lambda} \tag{7}$$

where q_i, $q_j \in V_Q$ and q'_λ, $q'_\eta \in V_{Q'}$ such that $(1 \leq i, j \leq n, 1 \leq \lambda, \eta \leq m)$. The normalization coefficient d_{qiqj} is required in the relaxation process to obtain the precise probability, such that $\sum_{j=1}^{n} d_{qiqj} = 1$. The support function provides matching probability information that requires further normalization and is given by:

$$p^{(1)}_{qi \to q'_\lambda} \leftarrow \frac{T_{qj}}{\sum_{j=1}^{m} d_{qiqj}} \tag{8}$$

$p^{(1)}_{qi \to q'_\lambda}$ reveals the preliminary matching matrix between V_Q and $V_{Q'}$ in terms of probabilities:

$$M^1_{qi \to q'_\lambda} = \begin{bmatrix} P^1_{1 \to 1} & \cdots & P^1_{1 \to n} \\ \vdots & \ddots & \vdots \\ P^1_{m \to 1} & \cdots & P^1_{m \to n} \end{bmatrix} \tag{9}$$

where $M^1_{qi \to q'_\lambda}$ probability matching matrix that represents the soft matching among points. In order to obtain the global consistency, the relaxation labelling process is carried out iteratively that updates the matching such that each element in $M^1_{qi \to q'_\lambda}$ becomes closer to 0 or 1. The iteration procedure

can be given by the following equations:

$$\psi^{k-1}_{qi\to q'_\lambda} = \sum_j \sum_\eta C_{qiqj}(q'_\lambda, q'_\eta)\, p^{k-1}_{qi\to q'_\lambda} \tag{10}$$

$$p^{k}_{qi\to q'_\lambda} = \frac{p^{k-1}_{qi\to q'_\lambda}\, \psi^{k-1}_{qi\to q'_\lambda}}{\sum_j p^{k-1}_{qi\to q'_\lambda}\, \psi^{k-1}_{qi\to q'_\lambda}} \tag{11}$$

$p^{k}_{qi\to q'_\lambda}$ provides the refined probability of matching point q_i with q'_λ, after $k$iterations, where the matching probability of each correspondence is linked with probabilities of other points. As the iteration progresses, the value of probability becomes higher for those points where it is also supported by other points combinations and approaches to zero otherwise.

C. CUR Decomposition for GM

Matrix decomposition provides an efficient way to solve the problem by decomposing it into low rank structures that can be processed separately, later resuming the outcomes approaching to produce the global solution corresponding to original raw-matrix. For graph matching problems, decomposition based methods such as dual decomposition [17], non-negative matrix factorization [20], [24] are applied to factorize the original graph into less complex small scale subgraphs, and then combine the subgraph solution.

For the conventional decomposition methods, it is required to solve the matrix inversion of size at least square times the number of samples. In this case the low rank computation still costs polynomial order time, which makes them restricted to small scale graphs only. Therefore, traditional approaches to decompose graph only work for limited set of energy functions that have a relatively small graph connection. For image correspondence problems it is required to perform graph matching on large number of points as images are quite rich in terms of contextual information.

1) Computing CUR Decomposition: Different from the graph decomposition perspective, we propose to address these limitations by introducing the graph sketching, in fact, matrix sketching [28], [29], to deal graph matching in better space time complexities [27]. The compatibility matrices can be efficiently computed and represented by their sketches in terms of product of matrices.The small approximated matrices preserve most of the characteristics of original matrices in terms of sparsity and actual geometric graph connections (edges). To make this work self-contained, we first present the prototype CUR matrix decomposition followed by advanced form and then link this formulation to solve the GM.

For an arbitrary $m \times n$ n rectangular matrix A, where m and n can be the aforementioned number of points in graphs. It is more feasible to sample the c columns of A, with sampling indices S_c to generate $C = AS_C \in R^{m\times c}$ at the same time sample r rows of A, with sampling S_R to produce $R = AS_R \in R^{r\times n}$, and interestingly sampling in both directions to yield the intersection matrix $U^* \in R^{c\times r}$ by solving the minimization problem:

$$U^* = \arg\min_U \|A - CUR\|_F^2 = C^+ A R^+ \tag{12}$$

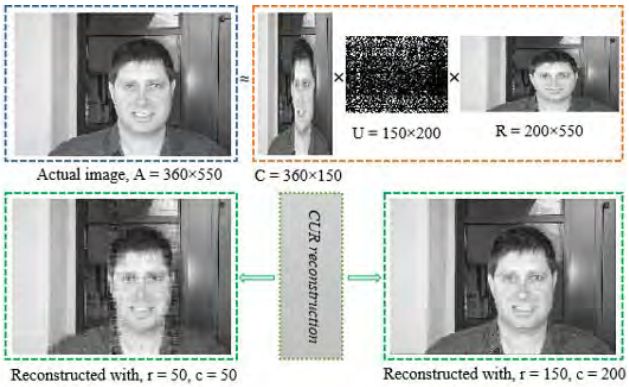

Fig. 3. An illustration of CUR decomposition on face image taken from [35] and its reconstruction using different numbers of selected rows and columns.

The low-rank approximation $A \approx CUR$ is termed as CUR decomposition [30]. In order to further demonstrate CUR factorization, consider Fig 3. as an example of a face image and its factorized parts. The purpose of CUR decomposition is to find a sub-image C (subset of columns of actual image), sub-image R (subset of rows of actual image), and compute U using the intersection of rows and columns, such that actual image can be reconstructed within the relative error.

Algorithm 1 CUR-Matching Matrix Approximation (MMA)

Input : Two graphs $V_Q(q_i \in V_Q : i = 1, 2, 3 \ldots, n)$ and $V_{Q'}(q'_\lambda \in V_{Q'} : \lambda = 1, 2, 3 \ldots, m)$
(2) Targeted number of rows c and column r
1: Compute partially observed compatibility coefficient matrices $C_{qiqj}(q'_\lambda, q'_\eta)S_C$, S_R, $S_{C,R}$
2: Initialize $p_{qi\to q'_\lambda}$ with prior probability
2: **Repeat** for $\mathbf{C}_{SC}$, $\mathbf{R}_{SR}$ and $\mathbf{U}_{SCSR}$
3:**For** each point (q_i, q_j)
4: $\psi^{k-1}_{qi\to q'_\lambda} = \sum_j \sum_\eta C_{qiqj}(q'_\lambda, q'_\eta)\, p^{(k-1)}_{qi\to q'_\lambda}$
5: $p^{(k)}_{qi\to q'_\lambda} = \frac{p^{k-1}_{qi\to q'_\lambda}\, \psi^{k-1}_{qi\to q'_\lambda}}{\sum_j p^{k-1}_{qi\to q'_\lambda}\, \psi^{k-1}_{qi\to q'_\lambda}}$
6: **end for**
5: **Until** Convergence
6: Approximate $\psi_{qi\to q'_\lambda} = \mathbf{C}_{SC}\mathbf{U}_{SCSR}$
7:**Output**: Matching matrix $X \in R^{m\times n}$

The small matrices hold direct representation from actual matrix, being very useful in solving assignment problem using the relaxation labelling, as the indices of sampled rows and columns are available ahead. For this prototype model the computation of sampled compatibility matrices might not be much advantageous, because U^* still needs to access every index of graph structure i.e. matrix A. Lately the faster version of CUR decomposition is proposed in [29] which differs in terms of forming the U^* matrix more efficiently. The column selection matrices $P_R \in R^{n\times p_r}$ and $P_C \in R^{m\times p_c}$ are generated through the sampled indices p_r and p_c with $p_c = p_r = O(c + r)$, so that enough approximation

is achieved.

$$U^{\sim} = \arg\min_{U} \|P_C^T A P_R - P_C^T C U R P_R\|_F^2 = (P_C^T C)^+ (P_C^T A P_R)(R P_R)^+ \quad (13)$$

The $U^{\approx}$ here require $P_C^T A P_R$ entries from large A instead of accessing the full matrix, as in the case of prototype model. Using the above formulation to compute the $U^{\approx}$ matrix allows the computation of large compatibility matrix in linear time with scale of graph. This feature allows the relaxation labelling optimization process to converge rapidly even in the presence of large-scale graphs as compared to baseline where the global solution is more challenging to achieve.

2) CUR for Matching Matrix Approximation (CURMMA): From graph matching perspective, the CUR decomposition first allows to compute only the sampled compatibility coefficients. Empirically, the sampling indices when generated through uniform sampling process behaves nearly like the well-known leverage score sampling matrices. Leverage score based sampling is expensive in terms of computing the SVD of whole dataset, whereas uniform sampling avoids computing every entry of matrix. The performance of uniform sampling is data dependent. However, for uniform leverage scores or small coherence matrices, uniform sampling provides a better sketch [31]. In our experiments, we used uniform sampling method explained in [29], to first oversample the entries and then reducing them with mutual repetition. The Eq. (3), can be rewritten by sampled factored matrices to approximate the solution as:

$$\hat{X} = \arg\max_{X} \sum_{(q_{\theta_T}, q'_{\theta_T}) \in C} f(\mathbf{C}_{S_C}, \mathbf{U}_{S_C S_R}, \mathbf{R}_{S_R}) \quad (14)$$

Given the number of selected rows r and columns c, we therefore computed three small sampled compatibility pairwise matrices, where sampled distance and angle coefficient are computed initially to produce the combined compatibility factor matrices as:

$$\mathbf{C}_{S_C} = \mathbf{C}_{qiqj}(q'_\lambda, q'_\eta) S_C \in R^{mn \times mc}$$
$$\mathbf{R}_{S_R} = \mathbf{C}_{qiqj}(q'_\lambda, q'_\eta) S_R \in R^{rn \times mn}, \text{and}$$
$$\mathbf{U}_{S_C S_R} = (P_C^T \mathbf{C}_{SC})^+ (P_C^T \mathbf{C}_{qiqj}(q'_\lambda, q'_\eta) P_R) \mathbf{R}_{SR} P_R)^+ \in R^{mc \times rn}$$

Here we make a key observation about sampling the compatibility matrix, which can be treated as reducing the geometric combinations, but the number of graph nodes remains unchanged. The matric $\mathbf{C}_{SC}$ intuitively represents the matching lines from objective graph to all nodes but few combinations which can be treated as reference landmark points for matching. Similarly, $\mathbf{R}_{SC}$ matrix represents the all nodes with few selected combinations to all target combination points, whereas the U serves the purpose of scaling the R matrix, such that the product of all approximates the all points to all point combination coefficients.

The above formulation described above for probability relaxation labelling process cannot be directly enforced on the sampling matrices, as the whole searching space is now altered. In this case the above relaxation labelling and update equations can be modified to replace the existing procedure as:

$$\psi^{k-1}_{qi \to q'_\lambda} S_{C,R} = \sum_{j=1}^{c} \sum_{\eta}^{r} \mathbf{C}_{qiqj} = (q'_\lambda, q'_\eta) S_{C,R} P^{(k-1) S_{C,R}}_{qi \to q'_\lambda} \quad (15)$$

$$P^{k}_{qi \to q'_\lambda} S_{C,R} = \frac{p^{k-1}_{qi \to q'_\lambda} \psi^{k-1}_{qi \to q'_\lambda} S_{C,R}}{\sum_j p^{k-1}_{qi \to q'_\lambda} \psi^{k-1}_{qi \to q'_\lambda} S_{C,R}} \quad (16)$$

The initial probability matrix is thus initialized accordingly with the newly constructed sampled compatibility scores, and therefore the labelling process computes support for match only for the designated branches. The overall matching matrix can be approximated by considering the fractional matching matrices in terms of $p^{(k)}_{qi \to q'_\lambda}$, $\mathbf{C}_{SC}$, $p^{(k)}_{qi \to q'_\lambda} \mathbf{R}_{SR}$ and $p^{(k)}_{qi \to q'_\lambda} \mathbf{U}_{S_C S_R}$, that present the fraction of entire matching space.

$$p^{(k)}_{qi \to q'_\lambda} = p^{(k)}_{qi \to q'_\lambda}, \mathbf{C}_{SC} p^{(k)}_{qi \to q'_\lambda} \mathbf{U}_{S_C S_R} p^{(k)}_{qi \to q'_\lambda} \mathbf{R}_{SR} \quad (17)$$

The above equation refers to the approximate solution to the large assignment matrix in terms of small fractional matched matrices. The above procedure to approximate the matching solution significantly reduces the complexity by limiting the search space and facilitates the global convergence. The matching matrix approximation assigns the estimated matching probability to every point corresponding to the target point.

Algorithm 2 CUR-Tensor Completion and Matching (TCM)

Input : Two graphs V_Q and $V_{Q'}$
(2) Targeted number of selected branches K and L
1: Compute partially observed tensor W and core tensor: $U = W \times_1 W^+_{(1)} \times_2 W^+_{(2)} \times_3 W^+_{(3)}$
2: Construct fibre matrices C_1, C_2, C_3, and C_4
3: Initialize $p_{qi \to q'_\lambda}$
4: **Repeat**
5:**For** each point (q_i, q_j)
6: Reconstruct tensor slice:
$Y_{ij} = U \times_1 C_{1i} \times_2 C_{2j} \times_3 C_3 \times_4 C_4$
7: $\psi^{k-1}_{qi \to q'_\lambda} = \sum_j \sum_\eta Y_{ij} p^{(k-1)}_{qi \to q'_\lambda}$
8: $p^{(k)}_{qi \to q'_\lambda} = \frac{p^{k-1}_{qi \to q'_\lambda} \psi^{k-1}_{qi \to q'_\lambda}}{\sum_j p^{k-1}_{qi \to q'_\lambda} \psi^{k-1}_{qi \to q'_\lambda}}$
9: **end for**
5: **Until** Convergence
7: Output: Assignment matrix $X \in R^{m \times n}$

3) CUR for Tensor Completion and Matching (CURTCM): The expression that arise from compatibility coefficient can be better understood using the multiway array or tensor, where the pairwise information of points is kept in each mode. For instance matching pairs $a = (q_i, q'_\lambda)$ with $b = (q_j, q'_\eta)$ having a compatibility score stored in $\mathbf{C}_{qiqj} = (q'_\lambda, q'_\eta)$, can be alternately expressed in a 4th order tensor form as $Y \in R^{I \times J \times K \times L}$, where I, J, K and L are the corresponding dimensions in each mode. One approach to render the problem of graph matching more tractable is to first approximate the

large compatibility tensor in terms of its mode matrices and core tensor as a partially observed incomplete tensor, rather than realizing a single large coefficient tensor. Later the final solution can be realized by reconstructing the tensor fibers for probability relaxation labelling in iterative manner.

Within the procedure only few branches of graphs are required to estimate the tensor and later CUR factorization can be used to approximate the large graph. Therefore, in the current scenario we propose to address the graph matching problem with compatibility tensor completion problem. It is assumed that, sampling only the branches form two graphs not reduce the computation cost and helps to avoid the redundant pairs, but also can overcome the effect of outliers while dealing with deformable graphs. The steps below present the multilinear extension of CUR decomposition for Graph matching problem along with relaxation labelling.

For the tensor CUR based graph completion and matching, the expression that arises form Eq. (4) by incorporating the multilinear extension of CUR decomposition, consists of mode matrices and a core tensor as: $A_1 \in R^{I\times R_1}$, $A_1 \in R^{I\times R_1}$, $A_1 \in R^{I\times R_1}$ tensor $A_1 \in R^{I\times R_1}$, such that:

$$Y = G \times_1 A_1 \times_2 A_2 \times_3 A_3 \times_4 A_4 \tag{18}$$

where, R_1, R_2, R_3 and R_4 are the number of selected indices corresponding to each dimension which equally resembles with the variables c and r in matrix case. For each dimension of tensor the selected indices sets can be given by: $I = [i_1, i_2, i_3 \ldots i_{R1}]$, $J = [j_1, j_2, j_3 \ldots j_{R2}]$, $K = [k_1, k_2, k_3 \ldots k_{R3}]$, $L = [l_1, l_2, l_3 \ldots l_{R4}]$ where, the indices I, J, K and L resembles with the p_r and p_c in matrix case. The unfolding matrices in each mode resulting from selected indices can be used to construct the core tensor U, as

$$U = W \times_1 W^{+}_{(1)} \times_2 W^{+}_{(2)} \times_2 W^{+}_{(3)} \tag{19}$$

where, $W = Y(I : J : K : L)$ is the intersection tensor computed through the sampling indices. The original tensor can be approximated by using the Tucker representation as:

$$Y = U \times_1 C_1 \times_2 C_2 \times_3 C_3 \times_4 C_4 \tag{20}$$

where $\mathbf{C}_1 \in R^{I\times R_2R_3R_4}$, $\mathbf{C}_2 \in R^{J\times R_2R_3R_4}$, $\mathbf{C}_3 \in R^{K\times R_2R_3R_4}$, $\mathbf{C}_4 \in R^{L\times R_2R_3R_4}$ and are formed by partially observing the coefficient tensor as $\mathbf{C}_1 = \mathbf{Y}_{(1)}(:, J : K : L)$, $\mathbf{C}_2 = \mathbf{Y}_{(3)}(:, I : J : L)$, $\mathbf{C}_3 = \mathbf{Y}_{(1)}(:, J : K : L)$ and $\mathbf{C}_4 = \mathbf{Y}_{(4)}(:, I : J : K)$.

This arrangement makes the sampling of graph connections more understandable, while keeping the first two dimension of tensor unchanged, and it is possible to reduce the graph branches. The graph structure in terms of compatibility coefficient in this case represents the small sampled mode matrices and subtensor. In order to achieve the matching matrix more efficiently, only the required tensor slice is reconstructed in relaxation labelling, such that each iteration goes on single reconstructed tensor slice, while the remaining tensor remains factorized. The algorithm is summarized in Algorithm 2.

4) Complexity: The proposed matching method is motivated by the random selection of rows and columns (graph edges). Specifically, the proposed method is only $O(c + r)$ space complexity rather than $o(m + n)$, from initial affinity matrix,

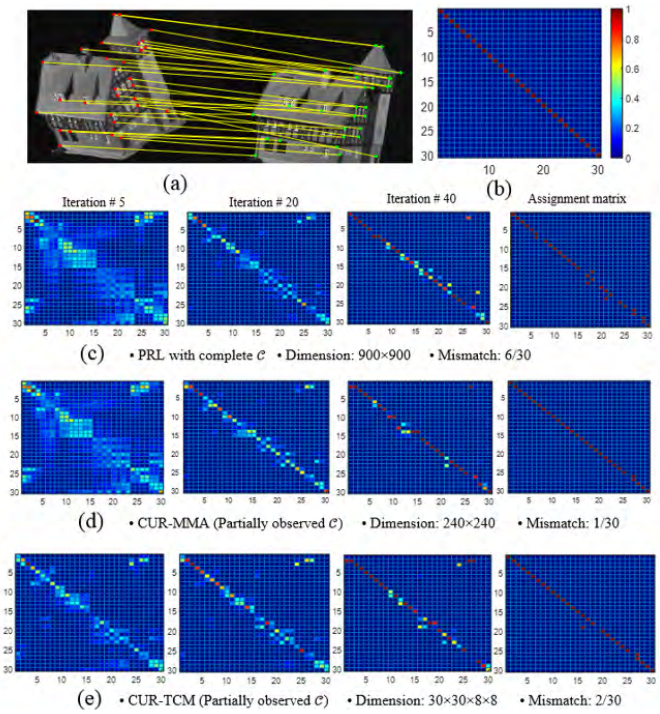

Fig. 4. The permutation matrix resulting from the baseline PRL and proposed methods CURMMA, CURTCM for a number of iteration are shown along with the size of compatibility matrix for relaxation labelling.

where, $c \ll m; r \ll n$. In addition, the time complexity of CURMMA is $o(m * n * c * r)$, which is much less than the baseline, i.e $o(m * n * c * r) = o(m^2 * n^2)$.

5) Approximate Discrete Solution and Sparsity: In our discussion, we emphasise on two variants of proposed approach in comparison to baseline method. As discussed earlier both CURMMA and CURTSTM can produce the approximate solution of relaxation labelling process. However, the major advantage not only lies in the robustness against outliers due to factorization but also can be seen in time consumption, sparsity and convergence. Interestingly, the CUR decomposition based approximate solution also converges to a local optimum with majority of elements either close to zero or one. The fact can be well understood by following example taken from the house dataset, where two images are matched based on their key points. The probability relaxation labelling process on raw compatibility matrix (considering all combinations) and the proposed methods CURMMA and CURTCM are shown below along with the corresponding dimensions of matrix (see Fig. 4). The convergence of the solution to local optimum is still achievable by using the proposed methods as the compatibility coefficients matrix retains their actual interpretation of positive numeric values along with actual graph edges. Moreover, the proposed methods can still return the permutation matrix comparable or better than baseline method while consuming only the partial structure of graph. Fig. 4 is presented from a CMU house dataset sample for illustration only. The matching lines corresponds to the geometric correspondence links to the nodes of the target graph. For PRL 900–900 matrix is required for pairwise matching labels, where as CURMMA and CURTCM require less than one third to produce better result and faster convergence.

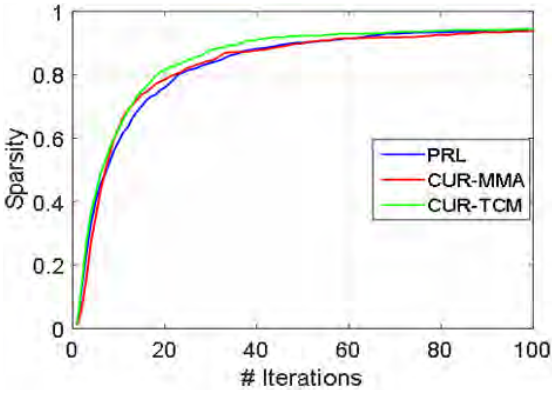

Fig. 5. The Sparsity comparison of the solution across the iterations in probability relaxation labelling.

We also present the sparsity when solving for matching correspondence for given point sets. Fig. 5 illustrates the matching process of synthetic point dataset of 98 points in 2D space. The sparsity with in the permutation matrix is computed per iteration for proposed methods and it can be seen that the CURTCM achieves relatively better or equivalent sparsity as compared to baseline.

V. Experiment Results and Analysis

In this section we evaluate the proposed method on several matching tasks, using both standard synthetic datasets and real-world images datasets. On real world images, the two variants of proposed approach named as CUR based matching matrix approximation (CURMMA) and CUR tensor based completion and matching (CURTCM) along with baseline probabilistic relaxation labelling (PRL) method are compared with the recent state of the art GM algorithms including, Spectral matching (SM) [6], the local sparse model matching (LSM) [7], adaptive graph matching (ADM) [5] and reweighted random walks matching algorithm (RRWM) [22]. The accuracy measure is adopted to evaluate the performance of all graph matching methods, i.e., the number of accurately detected matched pairs out of all available ground truth matched pairs.

Experiments are conducted on core i7 system with 16 GB memory. Our proposed methods, CURMMA and CURTCM along with the baseline PRL are implemented on Matlab environment, whereas SM, ADM, RRWM and LSM were accessed through public implementations. In our experiments we set the value of iteration to 40, whereas in CURMMA and CURTCM the values of c, (rows value), r (column value) and K, L are set empirically to 10% of the actual number respectively. The parameter settings of other algorithms are followed according to their studies.

A. Synthetic Dataset

The proposed method is first evaluated on the synthetic dataset [21], which refers to the shape of fish in 2D points. Each point set in the data set comprises of at least 98 points. Fig. 6 top row is the sample chosen from the deformation case which represents the matching by (a) PRL, (b) CURMMA and

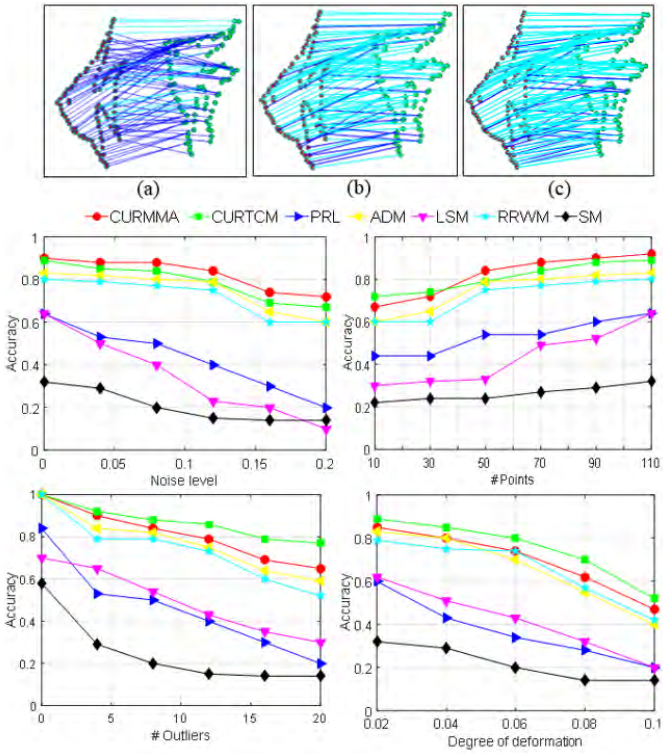

Fig. 6. The Matching comparison of different algorithms on synthetic dataset of 2D points, while considering number of factors such as noise, graph size, outliers and deformations. Top figures show the typical scenario of deformation (a) is baseline PRL, (b) is CUR-MMA and (c) is CURTCM. blue lines indicate the mismatches.

(c) CURTCM. The proposed method clearly achieves much better matching, as the blue line indicates the mismatching compared with ground truth. The bottom rows of Fig. 6 indicate the comparative performance against each challenging scenarios, such as noise, non-rigid deformation, outliers and problem size. The noise level of initial point set is varied from 0 to 0.2 with step size of 0.05 by adding Gaussian random noise. However, problem size is varied by considering only the subset of points by uniformly sampling the given and target points along with ground truths. For cases with outliers, point set ranging from 0 to 20 is produced by adding random points with normal distribution and unit variance whereas in deformation case, the target is deformed by adding non-rigid transformation and is varied from the scale of 0.02 to 0.1. The quantitative comparison reveals that the performance in each case is better against other algorithms. CURMMA is proved to be better in noise and problem size cases, where similar to outliers and deformation cases CURTCM leads the result. Interestingly as the number of points in problem size grows the result becomes better for almost all methods. This can be understood by the fact that, the sparseness of the graph is not strong enough to construct the true graph structure, whereas for sufficient number of points the ratio of noisy points decreases which makes it less susceptible to mismatches.

The effect of uniform sampling graph edges against the matching accuracy is depicted in Fig. 8, which shows that retaining 20 percent of edges can still produce better accuracy

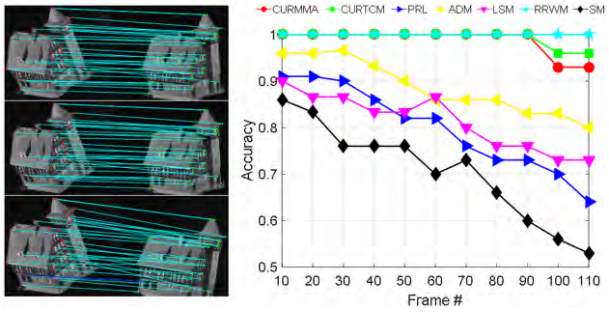

Fig. 7. The Comparison on House images sequence while matching initial frame with subsequent frames. The figures on left indicates the proposed method matching result on initial, middle and final frame.

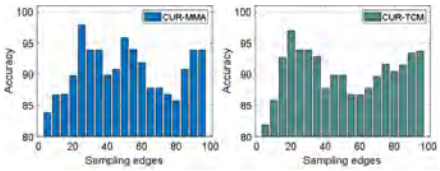

Fig. 8. Effect of sampling rate on matching accuracy on synthetic dataset using CUR-MMA (left) and CUR-TCM (right).

and comparatively better matching as the effect of outliers in relaxation labelling is minimized that are responsible for supporting the probability. Fig. 8 shows the matching accuracy on synthetic dataset that contains both noise and deformation, therefore retaining the minimum possible edges (20%-25%) reduces the entire noisy search space to small apace to support probability and decreases the ambiguities among nodes, therefore minimizes the effect of outliers that are responsible for supporting the probability

B. House Dataset

For real world images, the first dataset we consider is the CMU house dataset [16], [22], which is in fact the most commonly used dataset for validating GM methods. The dataset consists of 111 frames from a 3D rotating house shape video sequence. Each frame in sequence is manually labelled with 30 key points along with true matching result. As the video progresses, task of matching becomes more challenging, as the relative deformation varies intensely. We evaluated our proposed method on this dataset on the scale of varying relative frame number. The images shown in Fig. 7 represents the matching samples from proposed method CURTCM. The matching accuracy is 100% till frame number 90, afterward 1 out of 30 points is mismatched, whereas the graph below demonstrates the comparison on varying frame baseline. It can be observed that the RRWM in this dataset consistently achieves highest matching without any mismatch. The proposed CURTCM and CURMMA achieves second and third highest accuracies as compared to the rest of methods.

A typical matching result of house image pair with corresponding key points is shown in Fig. 10, column 1, whereas the average accuracies are reported in Table I.

C. Cars-Motorbike and Caltech-101 Images Dataset

In this experiment we evaluated our proposed methods on cars-motor bike dataset along with 30 pairs of Caltech-101

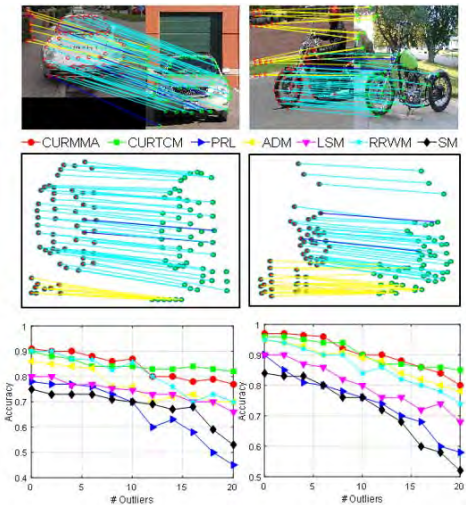

Fig. 9. Comparison of proposed method on Cars-motorbike dataset in the presence of outliers. The figures on left indicates the matching images with yellow lines indicating the outliers. Same points are drawn on 2D plane, which clearly indicates the matching of outliers outside the region occupied by main object.

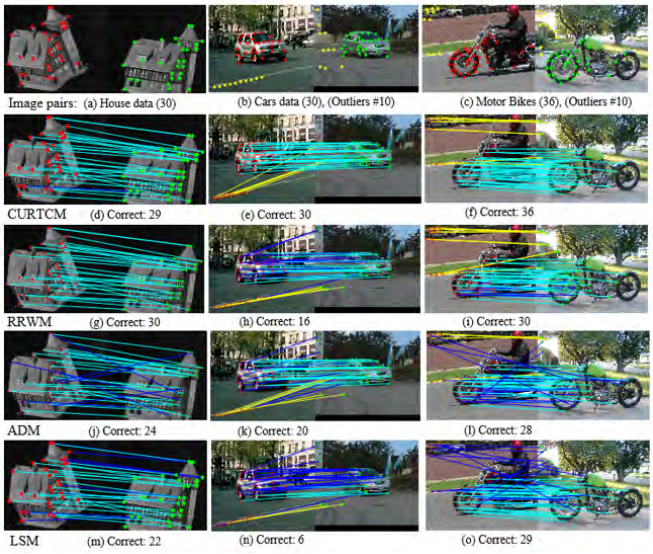

Fig. 10. Comparison Matching results of different algorithms on house sequence and Car-motorbike images. Top four algorithms are presented based on high matching results. Correct and wrong matches are represented by the magenta and blue colors respectively, whereas yellow lines indicate outliers.

images dataset presented in [35], which contains real images of cars, motorbikes and several other objects in different viewpoints, shapes, colour and background clutters. Images are arranged in 30 pairs of cars and 20 pairs of bikes along with number of extracted key points as inliers as well as outliers representing the background environment. The ground truths are available for inliers matching points. We compared the performance of each algorithm following the similar settings in [5], [22]. Fig. 9 shows the comparative results that are conducted by matching the inliers in both images while increasing the number of outliers from background, whereas the overall average accuracies of dataset are reported in Table II.

It can be seen that varying the number of outliers decreases the matching accuracy, as the ambiguities in extracting the

TABLE I
COMPARISON OF AVERAGE MATCHING ACCURACIES ON DIFFERENT DATASETS USED

Datasets	SM	PRL	LSM	RRWM	ADM	CURMMA	CURTCM
House	71.65	78.76	78.22	**100**	89.23	98.78	99.39
Synthtic	42.80	58.32	61.19	79.80	82.42	**84.23**	83.87
Car	0.7381	76.95	57.06	88.41	86.32	89.06	**90.24**
Motor bike	0.7764	82.44	64.65	0.9258	91.12	**93.71**	92.32
Caltech-101	52.08	56.60	59.32	64.54	60.28	68.14	**69.60**

Fig. 11. Results for the matching pair of real images taken from [24] (top 3 rows) and Caltech-101 dataset (bottom2 rows). Blue indicates the mismatch whereas yellow indicates the outliers.

TABLE II
COMPARISON OF COMPUTATION TIME (SECONDS) ON DIFFERENT DATASETS USED

Datasets	SM	PRL	LSM	RRWM	ADM	CURMMA	CURTCM
Airplanes	5.44	53.21	21.84	28.27	34.98	16.09	33.15
Face	61.71	230.24	131.76	178.34	210.44	78.11	151.25
Motorbike	17.61	105.8	38.43	54.40	76.21	29.34	47.68
Car	39.31	372.36	190.51	255.72	320.5	113.95	210.32
Bus	20.61	82.65	73.02	100.14	130.27	45.3	82.55

CURTCM both achieve comparable performance in the presence of outliers. CURTCM remains top as outlier number reaches to 20, which is around 45% of the inliers. A typical case is depicted in Fig. 9. The top rows, the background outliers are inconsistent in both images, which makes the two graph structures ambiguous in matching. For better view, the points from these image pairs are redrawn on 2D plane instead on images itself. It is obvious from the view that inliers are matched with corresponding inliers in second image without mismatching with outliers. In our method such as CURTCM, the partial graph observation limits the effect of outliers. In comparison, conducting the relaxation labelling procedure with the outliers achieves very low confidence score to be matched with inliers, and t inliers may match with outliers of the other image. Several other examples from this dataset are presented in Figs. 10(b) and 10(c), which show the actual points. The matched points in comparison with top selected algorithms is displayed in columns 2 and 3. It is evident from the figures that the proposed method consistently achieves better accuracy in the presence of outliers. In Table 2,

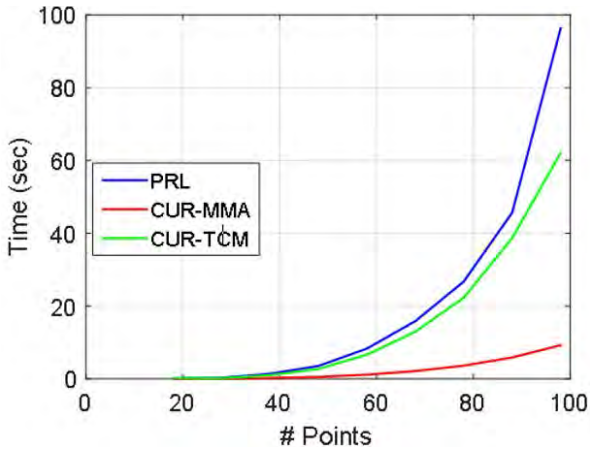

Fig. 12. Total time consumption for producing correspondence against varying number of graph edges.

we report the time comparison on different datasets. It can be seen that the proposed methods are efficient than the best performing methods RRWHM and ADM, and is slightly slower than but are much more accurate that the SM method. CUR based methods still achieve encouraging figures both in time and accuracy when compared to the baseline PRL method. Fig. 10, shows the effect of increasing the number of points on time cost in comparison with CUR factorization methods, which indicates the significant decrease in computation.

We further explored the image matching using the proposed method on different available natural images reported in recent studies [8]. The results are presented in Fig. 11, which indicates the robustness of proposed method in the presence of outliers. The interesting result can be seen in row 3 of Fig. 11, where the logo of bank is being matched in subsequent image. The outlier shares almost the same proportion with inliers, but accurate matching can still be obtained. Considering the conventional ways to build affinity matrix may lead to inconsistent result here due to high ratio of outliers. However, the sampling strategy to build tiny search space for edge computation and then recovering the complete graph structure here, minimizes the effect of these outliers.

D. Application on Non-Rigid Object Matching

Matching a non-rigid object i.e. an object moving in video, is much harder task as compared to pair of images discussed before. The fact can be better understood through an example given in Fig. 13. A tennis player moves within the video frames that not only change the structure of moving object but also alters the appearance of background accordingly. Under this situation the salient points extracted from images are no longer consistent as shown in top row of Fig 13. Graph matching in this context is even more challenging to cope with the scenario. To examine this issue, we have tested the proposed method on a video sequence taken from [8]. Salient points are first extracted from the video frames using the SURF feature point extractor. Fig. 13 shows the extracted feature

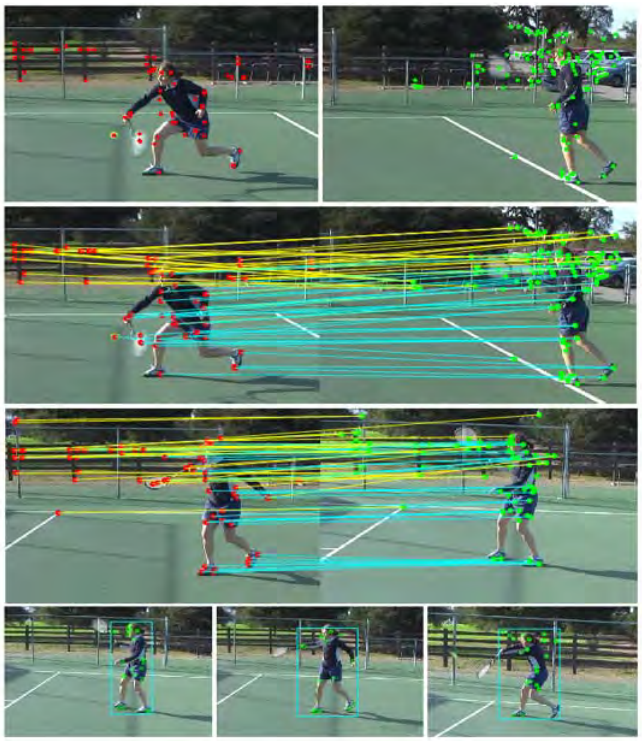

Fig. 13. An illustration of the application of CUR matching on video sequence with non-rigid motion of object.

points from different frames. It can be seen that the body motion and background variation make it harder to match the graph patterns, as the given points structure is inconsistent. The second row of Fig. 13 shows the matching result with a clear indication that the object matches with non-rigid object (cyan colour) in second image whereas the noisy background points are matched with each other (yellow colour).

The image correspondence problem can also be turned into an object tracking scenario, when the points of interest (inliers) are located in first image and then the corresponding match can be found. We also investigate this application by specifying the set of inliers in the first frame that corresponds only to the player. After matching the points between two frames with sufficient deformation and variations, we localize the object with the bounding box that represents the match with inliers only.

VI. Conclusion

In this paper, we have proposed CUR decomposition based graph matching framework and addressed image correspondence application. The technical crux of our study is the intuitive graph representation in terms of matrix approximation that is explicitly expressed as actual graph nodes and branches. The computation and accessibility to huge graph compatibility coefficient matrix is thus avoided by means of sampled small matrices in terms of CUR. Based on this key ingredient we proposed two variants of proposed approach and analysed their performance on image correspondence datasets. The proposed methods is proved to be robust against background outliers and the image deformations

caused by viewpoints. We demonstrated that the combination of approximating the matching with CUR decomposition and conducting relaxation labelling on sampled compatibility scorers has added robustness to final image correspondence. Moreover, the reduced size small C, U and R compatibility coefficients are much lighter to compute and store without any need of accessing the overweight compatibility matrix, as in case of traditional approaches where the inversion of such a large matrix is itself a time-consuming task. Considering the performance of proposed method in image correspondence problem, we would like to further investigate more deterministic way to choose b ranches optimally, while establishing prior CUR framework. Lastly, we aim to further extend this mathematical abstraction to higher order matching problems. We also conclude with the remarks that the heuristic variants of proposed methods can be extended to solve many complex image and video analysis problems with affordable space-time complexities.

REFERENCES

[1] W.-Z. Nie, A.-A. Liu, Y. Gao, and Y.-T. Su, "Hyper-clique graph matching and applications," *IEEE Trans. Circuits Syst. Video Technol.*, vol. 29, no. 6, pp. 1619–1630, Jun. 2018.

[2] H. Shang, Y. Tao, Y. Gao, C. Zhang, and X. Wang, "An improved invariant for matching molecular graphs based on VF2 algorithm," *IEEE Trans. Syst., Man, Cybern. Syst.*, vol. 45, no. 1, pp. 122–128, Jan. 2015.

[3] J. Xiao, H. Cheng, H. Sawhney, and F. Han, "Vehicle detection and tracking in wide field-of-view aerial video," in *Proc. IEEE Comput. Soc. Conf. Comput. Vis. Pattern Recognit.*, Jun. 2010, pp. 679–684.

[4] P. J. Besl and N. D. McKay, "Method for registration of 3-D shapes," *Proc. SPIE*, vol. 1611, pp. 586–607, Apr. 1992.

[5] X. Yang and Z.-Y. Liu, "Adaptive graph matching," *IEEE Trans. Cybern.*, vol. 48, no. 5, pp. 1432–1445, May 2018.

[6] M. Leordeanu and M. Hebert, "A spectral technique for correspondence problems using pairwise constraints," in *Proc. IEEE 10th Int. Conf. Comput. Vis. (ICCV)*, vol. 1, Oct. 2005, pp. 1482–1489.

[7] B. Jiang, J. Tang, C. Ding, and B. Luo, "A local sparse model for matching problem," in *Proc. AAAI 29th Conf. Artif. Intell.*, 2015, pp. 3790–3796.

[8] K. Jia *et al.*, "ROML: A robust feature correspondence approach for matching objects in a set of images," *Int. J. Comput. Vis.*, vol. 117, no. 2, pp. 173–197, 2016.

[9] J.-H. Lee and C.-H. Won, "Topology preserving relaxation labeling for nonrigid point matching," *IEEE Trans. Pattern Anal. Mach. Intell.*, vol. 33, no. 2, pp. 427–432, Feb. 2011.

[10] C. Cui, Q. Li, L. Qi, and H. Yan, "A quadratic penalty method for hypergraph matching," *J. Global Optim.*, vol. 70, no. 1, pp. 237–259, 2018.

[11] B. Jiang, J. Tang, A. Zheng, and B. Luo, "Image representation and matching with geometric-edge random structure graph," *Pattern Recognit. Lett.*, vol. 87, pp. 20–28, Feb. 2017.

[12] B. Jiang, J. Tang, X. Cao, and B. Luo, "Lagrangian relaxation graph matching," *Pattern Recognit.*, vol. 61, pp. 255–265, Jan. 2017.

[13] D. Knossow, A. Sharma, D. Mateus, and R. Horaud, "Inexact matching of large and sparse graphs using laplacian eigenvectors," in *Proc. Int. Workshop Graph-Based Represent. Pattern Recognit.* Berlin, Germany: Springer, 2009, pp. 144–153.

[14] H. F. Wang and E. R. Hancock, "Correspondence matching using kernel principal components analysis and label consistency constraints," *Pattern Recognit.*, vol. 39, no. 6, pp. 1012–1025, 2006.

[15] J. Yan, H. Xu, H. Zha, X. Yang, H. Liu, and S. Chu, "A matrix decomposition perspective to multiple graph matching," in *Proc. IEEE Int. Conf. Comput. Vis.*, Dec. 2015, pp. 199–207.

[16] F. Zhou and F. De La Torre, "Factorized graph matching," *IEEE Trans. Pattern Anal. Mach. Intell.*, vol. 38, no. 9, pp. 1774–1789, Sep. 2016.

[17] L. Torresani, V. Kolmogorov, and C. Rother, "A dual decomposition approach to feature correspondence," *IEEE Trans. Pattern Anal. Mach. Intell.*, vol. 35, no. 2, pp. 259–271, Feb. 2013.

[18] P. Swoboda, C. Rother, H. A. Alhaija, D. Kainmuller, and B. Savchynskyy, "A study of lagrangean decompositions and dual ascent solvers for graph matching," in *Proc. IEEE Conf. Comput. Vis. Pattern Recognit.*, 2017, pp. 1607–1616.

[19] S. Gold and A. Rangarajan, "A graduated assignment algorithm for graph matching," *IEEE Trans. Pattern Anal. Mach. Intell.*, vol. 18, no. 4, pp. 377–388, Apr. 1996.

[20] B. Jiang, J. Tang, C. Ding, and B. Luo, "Nonnegative orthogonal graph matching," in *Proc. 31st AAAI Conf. Artif. Intell.*, 2017, pp. 4089–4095.

[21] H. Chui and A. Rangarajan, "A new point matching algorithm for non-rigid registration," *Comput. Vis. Image Understand.*, vol. 89, nos. 2–3, pp. 114–141, Feb. 2003.

[22] M. Cho, J. Lee, and K. M. Lee, "Reweighted random walks for graph matching," in *Proc. European Conf. Comput. Vis.* Springer, 2010, pp. 492–505.

[23] R. Zhang and W. Wang, "Second- and high-order graph matching for correspondence problems," *IEEE Trans. Circuits Syst. Video Technol.*, vol. 28, no. 10, pp. 2978–2992, Oct. 2018.

[24] B. Jiang, H. Zhao, J. Tang, and B. Luo, "A sparse nonnegative matrix factorization technique for graph matching problems," *Pattern Recognit.*, vol. 47, no. 2, pp. 736–747, 2014.

[25] D. Cai, X. He, J. Han, and T. S. Huang, "Graph regularized nonnegative matrix factorization for data representation," *IEEE Trans. Pattern Anal. Mach. Intell.*, vol. 33, no. 8, pp. 1548–1560, Aug. 2011.

[26] A. Zanfir and C. Sminchisescu, "Deep learning of graph matching," in *Proc. IEEE Conf. Comput. Vis. Pattern Recognit.*, Jun. 2018, pp. 2684–2693.

[27] S. Voronin and P.-G. Martinsson, "Efficient algorithms for cur and interpolative matrix decompositions," *Adv. Comput. Math.*, vol. 43, no. 3, pp. 495–516, 2017.

[28] A. Aldroubi, K. Hamm, A. B. Koku, and A. Sekmen, "CUR decompositions, similarity matrices, and subspace clustering," 2017, *arXiv:1711.04178*. [Online]. Available: https://arxiv.org/abs/1711.04178

[29] S. Wang, Z. Zhang, and T. Zhang, "Towards more efficient SPSD matrix approximation and CUR matrix decomposition," *J. Mach. Learn. Res.*, vol. 17, no. 1, pp. 7329–7377, 2016.

[30] M. W. Mahoney, "Randomized algorithms for matrices and data," *Found. Trends Mach. Learn.*, vol. 3, no. 2, pp. 123–224, 2011.

[31] A. Gittens and M. W. Mahoney, "Revisiting the Nyström method for improved large-scale machine learning," *J. Mach. Learn. Res.*, vol. 17, no. 1, pp. 3977–4041, 2016.

[32] C. F. Caiafa and A. Cichocki, "Generalizing the column–row matrix decomposition to multi-way arrays," *Linear Algebra Appl.*, vol. 433, no. 3, pp. 557–573, 2010.

[33] M. W. Mahoney, M. Maggioni, and P. Drineas, "Tensor-CUR decompositions for tensor-based data," *SIAM J. Matrix Anal. Appl.*, vol. 30, no. 3, pp. 957–987, 2008.

[34] L. Chen, Z. Zhao, and H. Yan, "A probabilistic relaxation labeling (PRL) based method for C. Elegans cell tracking in microscopic image sequences," *IEEE J. Sel. Topics Signal Process.*, vol. 10, no. 1, pp. 185–192, 2015.

[35] M. Leordeanu, R. Sukthankar, and M. Hebert, "Unsupervised learning for graph matching," *Int. J. Comput. Vis.*, vol. 96, no. 1, pp. 28–45, Jan. 2012.

Sheheryar Khan received the Ph.D. degree in electrical engineering from the City University of Hong Kong in 2018, and the M.Sc. degree (Hons.) in signal processing from Lancaster University, U.K., in 2010. Before joining City University, he has served as a Lecturer with COMSATS University Islamabad, Pakistan. He also served as a Post-Doctoral Fellow at the City University of Hong Kong. His research interests include image processing, computer vision, and pattern recognition.

Mehmood Nawaz received the B.S. degree from Bahauddin Zakariya University, Multan, Pakistan, in 2012, and the M.Sc. degree from Shanghai Jiaotong University, China, in 2017. He is currently pursuing the Ph.D. degree with the Department of Electrical Engineering, City University of Hong Kong. His research interests include graph matching, image segmentation, shape matching, and pattern recognition.

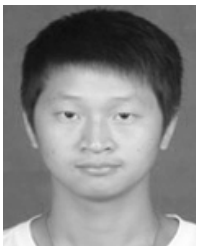

Xu Guoxia received the B.S. degree from the Department of Mathematics, Yancheng Teachers University, China, in 2015, and the M.S. degree from the College of Computer and Information, Hohai University, Nanjing, China, in 2018. He has also served as a Research Assistant in electrical engineering at the City University of Hong Kong. His research interests include image processing and computer vision.

Hong Yan (F'06) received the Ph.D. degree from Yale University. He was a Professor of imaging science at the University of Sydney. He is currently a Professor of computer engineering with the City University of Hong Kong. His research interests include image processing, pattern recognition, and bioinformatics. He has authored or coauthored over 600 journal and conference papers in these areas. He is a fellow of the IAPR. He was a recipient of the 2016 Norbert Wiener Award for contributions to image and biomolecular pattern recognition techniques from the IEEE SMC Society.